ENERGETIKA. 2015. T. 61. Nr. 3–4. P. 91–99

Molybdenum disulfide / mesoporous carbon nanocomposite as electrode material for supercapasitors

Lyudmyla Shyyko,

Volodymyr Kotsyubynsky,

Ivan Budzulyak,

Bogdan Rachiy

Vasyl Stefanyk Precarpathian National University, Shevchenko str. 57, 76018, Ivano-Frankivsk, Ukraine
E-mail liudmyla.shyiko@pu.if.ua

The article describes the features of MoS_2/mesoporous carbon nanocomposite creation and application as an electrode material for hybrid supercapacitors. The combination of these two materials improved the electrochemical characteristics in comparison with molybdenum disulphide or mesoporous carbon on their own; in particular the synergetic effect between them led to the reduction of internal resistance and increase of electric conductivity that are reflected in the maximum power of the capacitor. In spite of a large surface area of the mesoporous carbon obtained from the raw material of plant origin (2200 $m^2\ g^{-1}$), the synthesized nanocomposite (430 $m^2\ g^{-1}$) has almost twice higher specific capacity (57 Fg^{-1} and 110 Fg^{-1}, respectively) due to the summary effect of EDL and faradaic processes in the material. The samples were characterized by X-ray difractometry (XRD), transmission electron microscopy (TEM), porosimetry, impedance spectroscopy, voltammetry, and chronopotentiometry.

Key words: molybdenum disulfide, mesoporous carbon, hydrothermal synthesis, nanocomposite, hybrid supercapacitors

INTRODUCTION

Energy storage as well as its generation is an important issue in a whole set of industrial branches – beginning with the alternative energy sector and ending with automotive and portable everyday devices production. Supercapacitors as one of the solutions have occupied an important place in the scope of scientific interests. Owing to high power density, long cycle life, fast charge–discharge processes (within seconds) and small size, they have found implementation in electric and hybrid cars as a supplement to the existing battery due to their ability to take on large peak loads. In addition, they are used to start diesel and internal combustion engines, in the energy recovery systems of the electric rise in municipal electric transport, etc. Supercapacitors are a strategic product for improving the efficient use of electricity [1]. Electrochemical supercapacitors can operate on two principles, i. e. on adsorption of electrolyte ions on the electrode/electrolyte interface, the so-called electrical double-layer capacitors (EDLCs), and on fast and reversible faradaic redox reactions of electroactive materials that have several oxidation states or pseudocapacitance. In the first case, the main characteristic of electrochemical

double-layered or conventional supercapacitors is the value of specific surface area, which determines the amount of adsorbed ions. That is why researchers compete in methods of creating electrode materials with larger working surface, and as of today, the indisputable leader among them is carbon. Being low cost and environmentally friendly, it also has a variety of morphology, such as nanotubes (CNTs) [2, 3], graphene [4], mesoporous and thermally or chemically activated carbon [5], of which the last one possesses the highest specific surface area compared with other carbon materials [6]. However, owing to high power density and good reversibility that defines long working life, EDLCs have low energy densities. The second type – pseudocapacitors – operates through surface or bulk redox reactions, similar to Li-ion batteries with a very fast charge transfer between electrodes and electrolytes and can store more total energy than capacitors can.

However, in view of numerous applications of electronic devices and hybrid electric vehicles, there has been a great and urgent demand for high-performance energy storage devices with both high energy density and power density. The most intuitive approach to combine high energy and high power density within a single device is to combine the different types of energy storage sources. With a combination of the fast charging rate of SCs and high energy density of LIBs, a novel supercapacitor–battery hybrid energy storage system, also called hybrid supercapacitor (HSC), has emerged.

To unite the best features of both SCs and LIBs, it has been attempted to synthesize the MoS_2/mesoporous carbon nanocomposite and test it as an electrode material for supercapacitors. Charge storage in MoS_2 thin films can potentially occur via three main modes: 1) intersheet double-layer charge storage, 2) intrasheet double-layer charge storage on individual atomic MoS_2 layers via diffusion into the basal edges, and 3) faradaic charge transfer process on the Mo transition metal centre [7]. On the other hand, mesoporous carbon does not only have a large surface area providing the EDL capacity, but also keeps connected and prevents the exfoliation of MoS_2 during the charge/discharge process.

MATERIALS AND METHODS

Synthesis of MoS_2/C nanocomposite

The nanocomposite was synthesized via hydrothermal method using molybdate ammonium $(NH_4)_2MoS_4$ and hydrazine hydrate $N_2H_4 \cdot H_2O$ as precursors, surfactant cetyltrimethylammonium bromide $C_{19}H_{42}BrN$ as an additive agent, and pre-prepared mesoporous carbon obtained from the powder of ground apricot seeds mixed with 400 ml of 30% H_3PO_4 and thermally treated at the temperature of 550 °C in air. The reaction of hydrothermal procedure involved the reduction reaction of $[MoS_4]^{2-}$, the whole process lasted at 220 °C for 24 hours in a Teflon autoclave [8]. Additionally, the obtained material was annealed in argon atmosphere at 500 °C for 2 hours.

Material characterization

The synthesized material phase composition and structure were investigated by XRD (Cu K_α radiation). Morphological characteristics and chemical composition were obtained by TEM and EDS (FEI Technai G2 X-TWIN microscope). The specific surface area and pore size distribution were measured by nitrogen adsorption at 77.2 K (Quantachrome NOVA 2200e porosimeter). Before taking measurements, the samples were degassed at 180 °C for 18 h. The specific surface area (S_{BET}, $m^2\ g^{-1}$) was determined by the multipoint BET method. Electrical conductivity σ as a function of frequency was measured by the method of impedance spectroscopy in the frequency range of 0.01–100 kHz (Autolab PGSTAT 12/FRA-2 analyser); all samples were made in pellet form with the diameter of $17 \cdot 10^{-3}$ m and thickness of $0.1 \cdot 10^{-3}$ m under pressure of 34 MPa at the room temperature. Electrochemical tests were conducted in two electrode cells with galvanostatic and potentiodynamic cycling. The electrodes for EC were made as a mixture of <material> : <conductive additive (acetylene black)> : <PVDF> = 80:10:10. As an electrolyte, 1 M Na_2SO_3 aqueous solution was used.

RESULTS AND DISCUSSION

The XRD patterns of the synthesized material demonstrate the nearly X-ray amorphous state of the nanocomposite with only two present areas of

increased intensity of diffracted X-rays (Fig. 1). The (100) and (110) reflections at the angles 2θ of about 33.4 and 58.2° (Fig. 1a) have confirmed the formation of 2H-MoS_2 crystal structure, which belongs to the hexagonal system and P63/mmc symmetry group. The (002) peak in the vicinity of 2θ = 14–15° typical of this structure was not identified, which, according to [9, 10], indicates the lack of connection between the individual MoS_2 layers with the graphene-like structure.

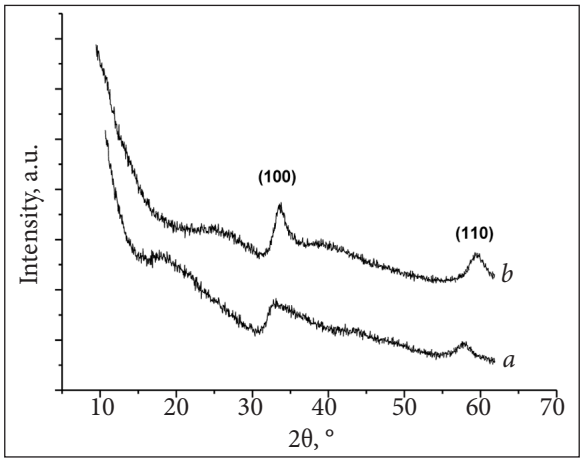

Fig. 1. Diffraction patterns of obtained materials after heat treatment at 80 ° (*a*), 500 °C (*b*)

Annealing in Ar atmosphere at 500 °C during 2 hours caused the exiguous shift of the reflection corresponded to the family of (110) planes, while the change in (100) reflection position was within acceptable error (Fig. 1b). This fact shows the change of interatomic distances within (001) plane, i. e. along the layers formed by Mo atoms placed between two layers of S atoms, forming a trigonal prism. But in general, it can be concluded that annealing did not significantly affect the morphology and composition of the nanocomposite.

The synthesized nanocomposite consists of stacked nanosheets (7–9) of MoS_2 characterized by crystalline order and dispersed in amorphous carbon (Fig. 2a–b). According to EDS analysis, the relative content of carbon atoms along the randomly chosen 2 μm line is at least 35 at.%, while that of Mo, S, and O is 15, 42, and 12 at.%, respectively.

The results of nitrogen sorption, in particular the pore size distribution of mesoporous

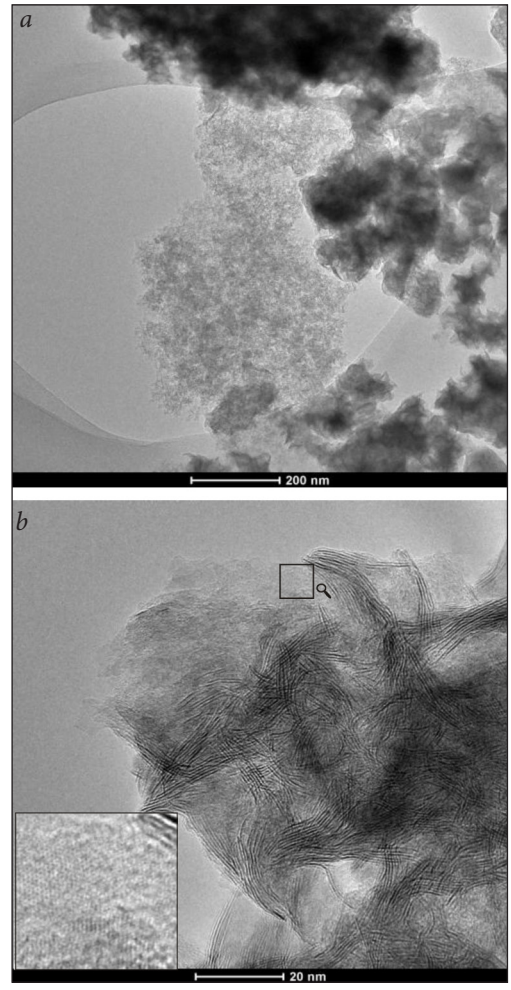

Fig. 2. TEM images of the material obtained by hydrothermal synthesis after heat treatment at 500 °C

carbon and synthesized nanocomposite (Fig. 3), confirmed that nanoparticles of molybdenum disulphide have localized in micro- and mesopores of carbon material. Comparing the pore size distributions of carbon and nanocomposite (cyan and blue colours in Fig. 3 online), one can see the difference in the pore width range of 0–8 nm. The surface areas, calculated by the BET method from nitrogen sorption curves, of mesoporous carbon and MoS_2/C nanocomposite are 2200 and 430 $m^2 g^{-1}$, respectively.

The frequency dependences of the complex conductivity for mesoporous carbon and nanocomposite MoS_2/C before and after annealing (Ar atmosphere at 500 °C for 2 hours) and also commercial MoS_2 (Merck KGaA) are presented in Fig. 4. The curves for all samples, except for commercial MoS_2, can be divided into two areas:

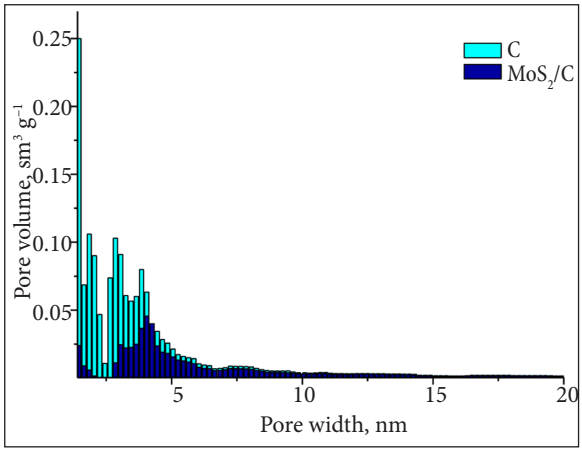

Fig. 3. (colour online) Pore size distributions for C and MoS_2/C

the linear frequency-independent region and the region where the conductivity increases sharply with the increase of frequency. Obtained dispersion curves were congruously approximated by Jonscher's power law in disordered materials (Eq. 1) [11]:

$$\sigma(\omega) = \sigma_{dc} + A\omega^n, \quad (1)$$

where σ_{dc} is frequency-independent part of conductivity, A is a temperature-dependent constant that gives information about the strength of the polarizability (or non-ideal conductivity), which comes from the diffusive motion of carriers in the sample. The exponent n is the slope of the linear section of the high-frequency dispersion (its value ranges from 0 to 1), and it describes the process of charge transfer in disordered materials and is a measure of the interaction between charged particles involved in the processes of polarization and conductivity, and also it depends on the temperature.

Table 1. **The data obtained from Jonscher's power law approximation**

Sample	A	n	σ_{dc}, Sm^{-1}
C	$5.4 \cdot 10^{-6}$	0.42	$1.1 \cdot 10^{-4}$
C (500 °C, Ar)	$7.6 \cdot 10^{-6}$	0.42	$1.8 \cdot 10^{-4}$
MoS_2/C	$2.0 \cdot 10^{-5}$	0.34	$4.8 \cdot 10^{-4}$
MoS_2/C (500 °C, Ar)	$2.7 \cdot 10^{-6}$	0.47	$5.1 \cdot 10^{-4}$

Table 1 gathers all data calculated from Jonscher's law approximation of experimental results. As it is presented, the conductivity for the direct current approximation of the synthesized nanocomposite is almost three times higher than that of mesoporous carbon used in the synthesis. Such low conductivity of mesoporous carbon is due to low ohmic contact between particles and carbon graphitization degree, and also due to the presence of oxygen-containing compounds on its surface that are formed mainly at the edges of graphite fragments, enlarging the barrier for

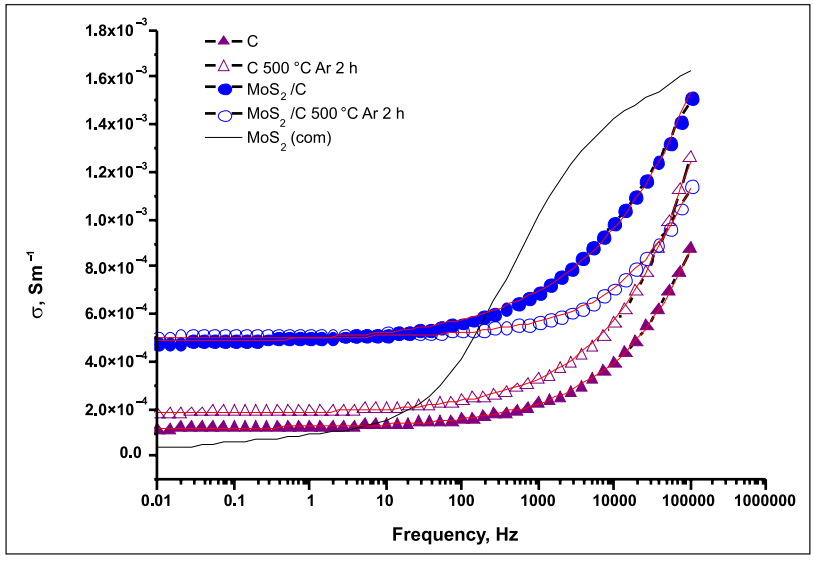

Fig. 4. Frequency-dependent electrical conductivity of the samples (solid lines represent the fitting results)

electron transfer from one crystal element to another [12]. At the same time, the nanocomposite possesses conductivity thirteen times higher than that of commercial MoS_2 with an average particle size of 10 μm (experimentally measured value in the same conditions is $0.38 \cdot 10^{-4}$ Sm^{-1}). The typical conductivity of MoS_2 is smaller and lies in the range of 10^{-6}–10^{-8} Sm^{-1} [11, 13]. The obtained result can be explained by a synergetic effect of the nanocomposite materials, carbon acts as a donor of electrons for molybdenum disulphide, which at low frequencies and at room temperature is usually *n*-type semiconductor with hopping conductivity, i. e. the exchange of electrons between Mo ions. The excess electrons from the electron donor would be expected to reduce the hardness of the electron transfer, and, according to [14], in the partial electron transfer from graphene (or carbon layer) to MoS_2 layers, each carbon atom donates ca. 0.027e to MoS_2 and the transferred electrons are located on sulphur atoms. In addition, the annealing leads to the sintering and tightness of the particles that improved contact between them.

As for the calculated values of *A* and *n* presented in Table 1 for today, the universal and exact relationship between these constants has not yet been defined, but by defining the slope *n*, some assumptions can be made about the charge carriers behaviour in the material. Jonscher suggested that the range of $0 < n < 0.4$ [15] corresponds to material conductivity based on the existence of conducting grains separated by less conducting barriers that behave as macroscopic dipoles strongly interacting with their neighbours, giving rise to a strong dispersion [16]. While the range of the exponent $0.4 < n < 0.6$ suggests multipolaron hopping of charge carriers across the interfaces of grains and grain boundaries or at the layers interfaces. This indicated the localized nature of the electronic charge carriers about the ionic sites of the crystal structure [17].

The improvement of the electrical properties is also demonstrated by electrochemical tests of supercapacitors with electrode material based on the synthesized nanocomposite. The chare/discharge galvanostatic measurements in a symmetrical two-electrode cell show the voltage drop ΔU, which determines the internal resistance *R* or equivalent series resistance (ESR) [6] of the electrode material made of mesoporous carbon (Fig. 5b):

$$R = \frac{\Delta U}{I}. \tag{2}$$

It in turn limits the maximum power of the capacitor [6]:

$$P_{\max} = \frac{U^2}{4R}. \tag{3}$$

The specific capacity was calculated by means of the formula:

$$C = \frac{2It}{(U_m - \Delta U)m}, \tag{4}$$

where *I* is a charge/discharge current, *t* is the discharge time, U_m is the maximum voltage, ΔU is

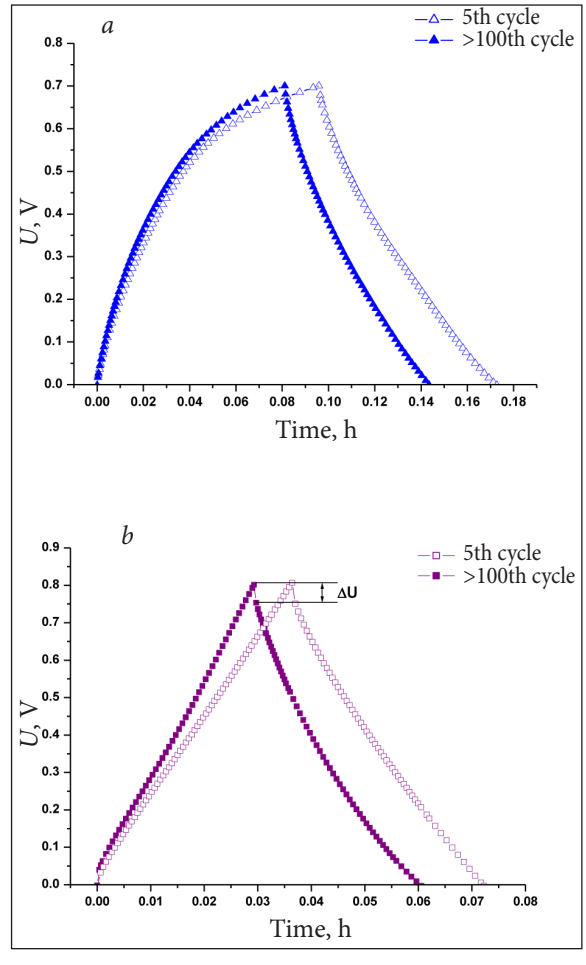

Fig. 5. Charge/discharge curves for MoS_2/C (*a*) and mesoporous carbon (*b*) at halvanostatic mode

the voltage drop at the closure of the discharge circle, and *m* is weight of the material. At the initial cycles, the specific capacity of the synthesized composite was 110 Fg^{-1}, and at the end it decreased to 90 Fg^{-1}; the calculated Columbic efficiencies were 80.2 and 77.8%, respectively. For mesoporous carbon, these values are smaller and equal 57.5 and 50.9 Fg^{-1}, but the efficiency increases from 94.5 up to 96.8%.

As a result, fast Faradic processes on the surface of MoS_2-based electrode material cause the overall capacity increase almost twice as compared to the carbon-based system. On the CV curves (Fig. 6a) at the sweep rate of 1 m Vs^{-1} in the potential window of 0–0.7 V, cathodic branch has a broad peak at 0.17 V for MoS_2/C, which blurred with the increase of the sweep rate (Fig. 6b), while the C-based electrochemical cell stayed close to rectangular shape.

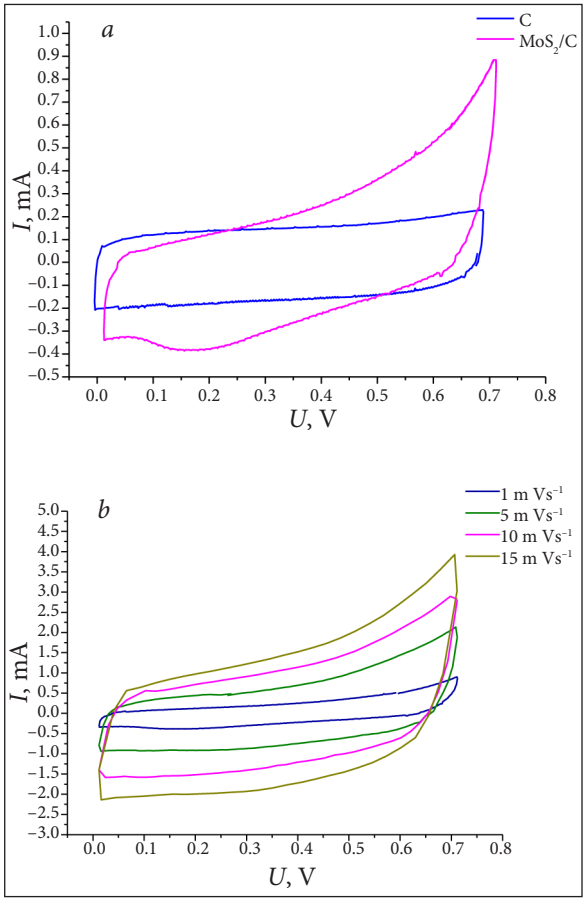

Fig. 6. (colour online) Cyclic voltammograms for MoS_2/C and mesoporous carbon-based systems at 1 m Vs^{-1} (*a*) and for MoS_2/C at different sweep rates (*b*)

To establish the electrochemical behaviour of the nanocomposite in aqueous electrolyte, Nyquist plots with the impedance spectroscopy method were chosen (Fig. 7). The curves fitting allowed picking up the elements of equivalent electrical circuit (EEC) (Fig. 7a–b). In general, the equivalent circuit assemblage is close to the results presented by Zhibin et al. [18].

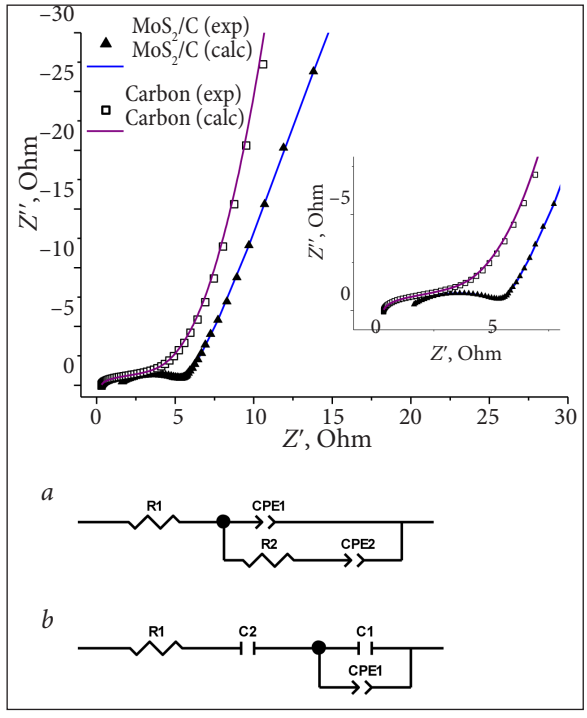

Fig. 7. Experimental and calculated Nyquist plots of the symmetric supercapacitors based on MoS_2/C and mesoporous carbon in 1 M 1 M Na_2SO_3 (aqueous). Equivalent circuit model used for fitting experimental data: for MoS_2/C (*a*) and mesoporous carbon (*b*)

The reaction resistances for the MoS_2/C-based system are given in Table 2. Here, R1 corresponds to the bulk resistance in the high-frequency region, which includes the electric resistance of the active material, contact resistance with the current collector, and electrolyte resistance. R2 contains the charge transfer reaction resistance in the high-to-medium-frequency region, where an electron is inserted from the external circuit into MoS_2, and in order to maintain the charge balance followed by the Na^+ ion insertion reaction. The straight-line sections with slopes of 71° in the low-frequency region

Table 2. **The data for EEC elements (MoS_2/C-based system)**

	R1	CPE1-T	CPE1-P	R2	CPE2-T	CPE2-P
Value	1.163	0.004	0.447	4.926	0.108	0.821
Error	0.098	0.0007	0.023	0.193	0.0015	0.009

Table 3. **The data for EEC elements (mesoporous carbon-based system)**

	R1	C2	C1	CPE1-T	CPE1-P
Value	0.332	0.183	0.00008	0.132	0.226
Error	0.006	0.004	0.000003	0.0035	0.004

correspond to the ionic diffusion of Na^+ ions in the electrode [20–22], where the presence of the semi-infinite linear diffusion is observed as linear relationship on the Bode plot (log|Z| vs log(ω). Analysing the obtained through approximation CPE1-P, taking into account the surface inhomogenity [21], one can conclude that CPE1 is close to the Warburg element with the value of 0.004 Ohm^{-1} (CPE1-T) referring to the diffusion of ionic species across the electrolyte/electrode interface. Thereby, CPE2-P is close to 1 indicating the pure capacitor behaviour with charge accumulation at EDL.

In the case of a symmetric supercapacitor with mesoporous carbon-based electrodes, the semicircle in the high-frequency region of the Nyquist plot is not observed, the slope angle of low-frequency branches of the Z′(-Z′′) dependence is relatively larger but less than 90°, indicating the presence of the charge accumulation processes different from the adsorption on EDL. The best result of Nyquist plot modelling was obtained with the equivalent circuit that contains series-connected capacitances, one of which is connected in parallel to an element of the constant phase (Fig. 8b). The value of CPE1-P determines the proximity of this element to resistance that can be explained by the electrode porosity. Such equivalent circuit, which includes parallel connected resistance and capacitance, corresponds to the usual EDL capacitors [6].

CONCLUSIONS

As a conclusion, it can be said that the combination of a large surface area of mesoporous carbon and fast Faradic processes in MoS_2 is a good solution for improving the working characteristics of supercapacitors. Despite that the surface area of the nanocomposite is much smaller than that of mesoporous carbon (430 and 2200 $m^2\ g^{-1}$, respectively), due to redox reactions occurrence in MoS_2, the resulting specific capacity of the nanocomposite is twice higher in comparison with just carbon. In addition, the synergetic effect between C and MoS_2 increases the electric conductivity of the synthesized material, because of the sum of hopping charge transfer mechanism on Mo atoms and additional electron donation by carbon atoms. In general, a simple and cheap method of MoS_2/C nanocomposite obtainment and a relatively good electrochemical performance made it a promising electrode material for supercapacitors.

Received 1 October 2015
Accepted 2 December 2015

References

1. Inagaki M., Konno H., Tanaike O. Carbon materials for electrochemical capacitors. *Journal of Power Sources*. 2010. Vol. 195. P. 7880–903.
2. An K. H., Jeon K. K. et al. High-capacitance supercapacitor using a nanocomposite electrode of single-walled carbon nanotube and polypyrrole. *Journal of the Electrochemical Society.* 2002. Vol. 149. No. 8. P. A1058–A1062.
3. Frackowiak E., Beguin F. Carbon materials for the electrochemical storage of energy in capacitors. *Carbon*. 2001. Vol. 39. No. 6. P. 937–950.
4. Brownson D. A. C., Banks C. E. Fabricating graphene supercapacitors: highlighting the impact

of surfactants and moieties. *Chemical Communications*. 2012. Vol. 48. P. 1425–1427.

5. Ostafiychuk B. K., Budzulyak I. M., Rachiy B. I., Vashchynsky V. M., Mandzyuk V. I., Lisovsky R. P., Shyyko L. O. Thermochemically activated carbon as an electrode material for supercapacitors. *Nanoscale Research Letters*. 2015. DOI 10.1186/s11671-015-0762-1.
6. Halper M. S., Ellenbogen J. C. *Supercapacitors: A brief overview*. The MITRE Corporation, McLean, Virginia, USA, 2006. 1–34 p.
7. Soon J. M., Loh K. P. Electrochemical double-layer capacitance of MoS_2 nanowall films. *Electrochemical and Solid-State Letters*. 2007. Vol. 11 A. P. 250–254.
8. Shyyko L. O., Kotsyubynsky V. O., Budzulyak I. M., Rawski M., Kulyk Y. O., Lisovski R. P. Synthesis and double-hierarchical structure of MoS_2/C nanospheres. *Physica Status Solidi A*. 2015, DOI: 10.1002/pssa.201532136.
9. Liang K., Chianelli R., Chien F., Moss S. Structure of poorly crystalline MoS_2 – A modeling study. *Journal of Non-Crystalline Solids*. 1986. Vol. 79. No. 3. P. 251–273.
10. Kun C., Chen W., *Journal of Materials Chemistry*. 2011. Vol. 21. P. 17075.
11. Ahmad M., Rafiq M., Imran Z., Rasool K., Shahid R, Javed Y., Hasan M. Charge conduction and relaxation in MoS_2 nanoflakes synthesized by simple solid state reaction. *Journal of Applied Physics*. 2013. Vol. 114. No. 4. P. 043710.
12. Biniak S., Swiatkowski A., Pakula M. *Chemistry and Physics of Carbon*. New York: Marcel Dekker. 2001, 125 p. ISBN 0-8247-0246-8.
13. Benavente E., Santa Ana M., Gonzalez G. Electrical conductivity of MoS_2 based organic–inorganic nanocomposites. *Physica Status Solidi B*. 2004. Vol. 241. No. 10. P. 2444–2447.
14. Koroteev V., Bulusheva L., Asanov I., Shlyakova E., Vyalikh D., Okotrub A. Charge transfer in the MoS_2/carbon nanotube composite. *The Journal of Physical Chemistry*. 2011. Vol. 115. No. 43. P. 21199–21204.
15. Jonscher A. Frequency-dependence of conductivity in hopping systems. *Journal of Non-Crystalline Solids*. 1972. Vol. 8. No. 10. P. 293–315.
16. Fourrier-Lamer A., Fizazi A., Belhadj-Tahar N. Studies of semiconducting organic polymer-graphite composites from d.c. to microwave frequencies. *Synthetic Metals*. 1988. Vol. 24. P. 95–105.
17. Naresh N., Bhrowmik R. Structural, magnetic and electrical study of nano-structured α-$Fe_{1.4}Ti_{0.6}O_3$. *Journal of Physics and Chemistry of Solids*. 2012. Vol. 73. No. 2. P. 330–337.
18. Zhibin L., Zhang J., Zhao X. S. Ultrathin MnO_2 nanofibers grown on graphitic carbon spheres as high-performance asymmetric supercapacitor electrodes. *Journal of Materials Chemistry*. 2012. Vol. 22. P. 153–160.
19. Atlung S., Jacobsen T. On the *ac*-impedance of electroactive powders. γ-manganese dioxide. *Electrochimica Acta*. 1976. Vol. 21. P. 575–584.
20. Qu D. Application of a.c. impedance technique to the study of the proton diffusion process in the porous MnO_2 electrode. *Electrochimica Acta*. 2003. Vol. 48. P. 1675–1684.
21. Jorcin J. B., Orazemb M. E., NadinePebere N. P., Tribollet B. CPE analysis by local electrochemical impedance spectroscopy. *Electrochimica Acta*. 2006. Vol. 51. P. 1473–1479.
22. Zhu Ch., Mu X., Van Aken P. A., Yu Y., Maier J. Single-layered ultrasmall nanoplates of MoS_2 embedded in carbon nanofibers with excellent electrochemical performance for lithium and sodium storage. *Angewandte Chemie International Edition*. 2014. Vol. 53. No. 8. P. 2152–2156.

Lyudmyla Shyyko, Volodymyr Kotsyubynsky, Ivan Budzulyak, Bogdan Rachiy

MOLIBDENO DISULFIDAS / MEZOPORINĖS ANGLIES NANOKOMPOZITAS KAIP ELEKTRODŲ MEDŽIAGA SUPERKONDENSATORIAMS

Santrauka

Straipsnyje aprašomos MoS_2/mezoporinės anglies nanokompozito sudarymo savybės ir elektrodų medžiagos taikymas hibridiniams superkondensatoriams. Šių dviejų medžiagų kombinavimas leidžia pagerinti elektrochemines savybes atskirai lyginant su molibdeno disulfidu ar mezoporine anglimi. Sąveikos / sinergijos poveikis lėmė vidinės varžos sumažėjimą ir elektros laidumo padidėjimą, tai leidžia pasiekti maksimalią kondensatoriaus talpą. Nepaisant didelio mezoporinės anglies, gautos iš augalinės kilmės žaliavos (2 200 $m^2\ g^{-1}$), savitojo paviršiaus ploto, susintetintas nanokompozitas (430 $m^2\ g^{-1}$) pasižymi beveik dvigubai didesne specifine talpa (atitinkamai 57 ir 110 Fg^{-1}) dėl EDL ir indukcinių procesų sinerginio poveikio. Mėginiai buvo tiriami naudojant rentgeno difraktometriją (XRD), perdavimo elektronų mikroskopiją (TEM), poringumą, impedanso spektroskopiją, voltametriją ir chronopotentometriją.

Raktažodžiai: molibdeno disulfidas, mezoporinė anglis, hidroterminė sintezė, nanokompozitas, hibridiniai superkondensatoriai